View metadata, citation and similar papers at core.ac.uk

brought to you by CORE

provided by HKU Scholars Hub

The HKU Scholars Hub The University of Hong Kong 香港大學學術庫

Title	Integrated energy management of plug-in electric vehicles in power grid with renewables
Author(s)	Gao, S; Chau, KT; Liu, C; Wu, D; Chan, CC
Citation	IEEE Transactions on Vehicular Technology, 2014, v. 63 n. 7, p. 3019-3027
Issued Date	2014
URL	http://hdl.handle.net/10722/216928
Rights	IEEE Transactions on Vehicular Technology. Copyright © IEEE.

Integrated Energy Management of Plug-in Electric Vehicles in Power Grid With Renewables

Shuang Gao, *Student Member, IEEE*, K. T. Chau, *Fellow, IEEE*, Chunhua Liu, *Senior Member, IEEE*, Diyun Wu, *Student Member, IEEE*, and C. C. Chan, *Fellow, IEEE*

***Abstract*—This paper presents an integrated control scheme for vehicle-to-grid (V2G) operation in the distribution grid with renewable energy sources. A hierarchical framework is proposed for V2G applications, and the mathematical models are built for both smart charging and V2G operation with distribution grid constraints. V2G power is regulated to minimize the total operating cost (TOC) while providing frequency regulation. The simulation results verify the control algorithm in coordinating distributed electric vehicle (EV) aggregations with the varying wind power and daily load. For V2G dynamic regulation, EVs connected in close proximity to wind power generators can locally compensate for the wind fluctuation with fast response and, hence, smooth out the power fluctuation at the bus having wind power generators and EVs. Each individual EV is strategically assigned to implement the simulated control algorithm through a bidirectional converter. An experimental platform is incorporated into the proposed integrated energy management to demonstrate the instantaneous response of EV battery storage.**

***Index Terms*—Dynamic regulation, electric vehicles (EVs), energy management, power grid, renewable energy, vehicle-to-grid (V2G).**

I. Introduction

TO COPE with the global energy crisis and environmental pollution, it is becoming desirable to integrate renewable energy generation such as wind power and solar power into the existing power grid. Meanwhile, electric vehicles (EVs), particularly the plug-in hybrid EVs, for green transportation have attracted increasing attention [1]. Because of the intermittent nature of wind power, large-scale integration of wind power poses a challenge on the power grid in both transient and steady states. Vehicle-to-grid (V2G) operation can help address the challenges by acting as a mobile energy storage device [1], [2].

EVs were simply regarded as dispatchable peaking power plants to participate in the unit commitment planning in [3]. A large number of EVs were considered adjustable generators, which were used to provide power to minimize both cost and emission. However, the characteristics of the V2G power and the location of EVs were not sufficiently considered in the V2G optimization model. Then, the feasibility analysis of EVs was conducted, which considered the limitations imposed on the V2G power due to the characteristics of EV batteries [4]. Moreover, a methodology for optimal charging sequence of EVs with aggregator control was proposed to maximize the V2G profit [5]. However, there were shortcomings that the power flow of EVs was unidirectional, the charging rate was fixed at the maximum limit, and the optimal solution was the selected charging intervals during the plug-in period.

With the ever-increasing popularity of EVs [6], the frequency regulation provided by V2G operation has been actively investigated. Several EV aggregations of different sizes and configurations were controlled in response to the frequency deviation signal [7]. Moreover, EVs could provide various auxiliary services such as the energy scheduling for load leveling [8], the minimization of charging cost [9], and the spinning reserve [10]. Although a variety of regulation services are suggested for V2G energy management, the multiobjective control method to manage EV energy for multiple ancillary services is absent in the literature.

The purpose of this paper is to develop a multilevel control structure for the distribution grid, which includes renewable energy sources and EVs, so that the V2G power can be properly deployed. The scale of distributed generators and the EV penetration degree are assumed for exemplification. Nevertheless, both the scale level and penetration degree can readily be modified for other case studies.

This paper is organized as follows. Section II presents the multilevel V2G framework where the widespread EVs are aggregated at different locations and microgrids. Another target is to establish a generic model for EV aggregations in different charging scenarios. Section III describes the optimal control algorithm that makes use of the scheduling of V2G power to minimize the operating cost. Section IV discusses the dispatching method of EVs to realize a multipurpose utilization of V2G power. Furthermore, a downscaled experimental setup is built to implement the dispatching method. Finally, the proposed control scheme is summarized, and a conclusion is drawn in Section V.

II. Modern Power Grid for Electric Vehicle Integration

A. Updated Power Grid With New Components

The conventional resource-centric control model of the power system is no longer sustainable; thus, a V2G control

Manuscript received September 9, 2013; revised February 5, 2014; accepted March 12, 2014. Date of publication April 8, 2014; date of current version September 11, 2014. This work was supported in part by the Basic Research Program of the Science, Technology, and Innovation Commission of Shenzhen Municipality under Project JCYJ 20120831142942515 and in part by the University Research Grants of The University of Hong Kong under Project 201210159060. The review of this paper was coordinated by Dr. A. Davoudi.

The authors are with the Department of Electrical and Electronic Engineering, The University of Hong Kong, Hong Kong (e-mail: ktchau@eee.hku.hk).

Color versions of one or more of the figures in this paper are available online at http://ieeexplore.ieee.org.

Digital Object Identifier 10.1109/TVT.2014.2316153

0018-9545 © 2014 IEEE. Personal use is permitted, but republication/redistribution requires IEEE permission.
See http://www.ieee.org/publications_standards/publications/rights/index.html for more information.

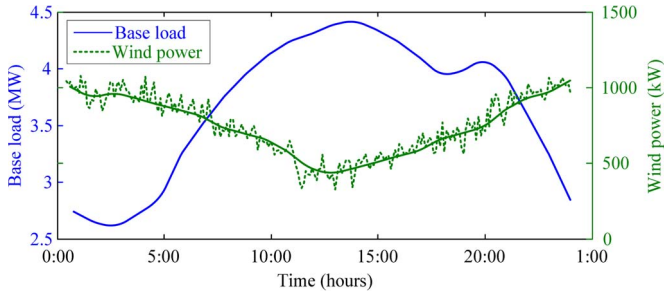

Fig. 1. Daily profiles of wind power generation and demand.

framework is proposed for the modern distribution grid, which incorporates new electric components, including renewable energy sources, microgrids, and adjustable electric appliances at the user end [1]. Energy storage devices are required in the power grid with large penetration of intermittent renewable energy sources. The widespread EVs in the power grid have good prospects of acting as distributed energy storage due to the sufficient power capacity from a large number of EV onboard batteries and the flexible power control provided by modern power electronic chargers. The EV aggregator assembles the power from a number of EVs and interacts with the grid operator through a two-way communication network. The aggregator is also responsible for dispatching the V2G power to each individual EV and monitoring the EV battery status. Furthermore, as an important energy storage device in microgrids, EVs react to the intermittent wind power and stabilize the power fluctuation at the common coupling point of microgrids.

The V2G control framework described in our previous paper [1] has been proposed within the existing structure of the power grid. The power drawn from the transmission network is delivered to the downstream electric consumers. A 33-bus distribution power network [11] is taken as an example, with wind power plants installed and placed on the selected buses. The total power supply from wind power is assumed 20% and evenly split into two wind power buses. The time-varying daily load and the typical wind power pattern with continuous small fluctuation are shown in Fig. 1. The variation of wind power generation profile opposes the load demand. Thus, the wind power generation exacerbates the unbalance between power supply and demand.

A number of EVs are plugged into the test power network through various charging infrastructures, such as the large charging stations with fast dc charging capability, the normal ac charging stations, and the domestic chargers. The charging infrastructures are assumed to cover about 20% of the region; the number of buses with EVs can be represented by $n_x = \mathrm{int}(r_{\mathrm{EV}} n_b) = 6$, where n_b is the total bus number, and r_{EV} is the spatial penetration degree of EVs. Thus, the charging load of EVs is superimposed to six buses, which are randomly selected.

B. V2G Scenario

The average percentage of vehicles parked at home through a day is derived from the 2009 National Household Travel Survey (NHTS) data, as shown in Fig. 2(a) [12]. It is shown that more than 90% of vehicles are parked at home between 9:00 P.M. to 6:00 A.M. In this home-charging scenario, it is assumed

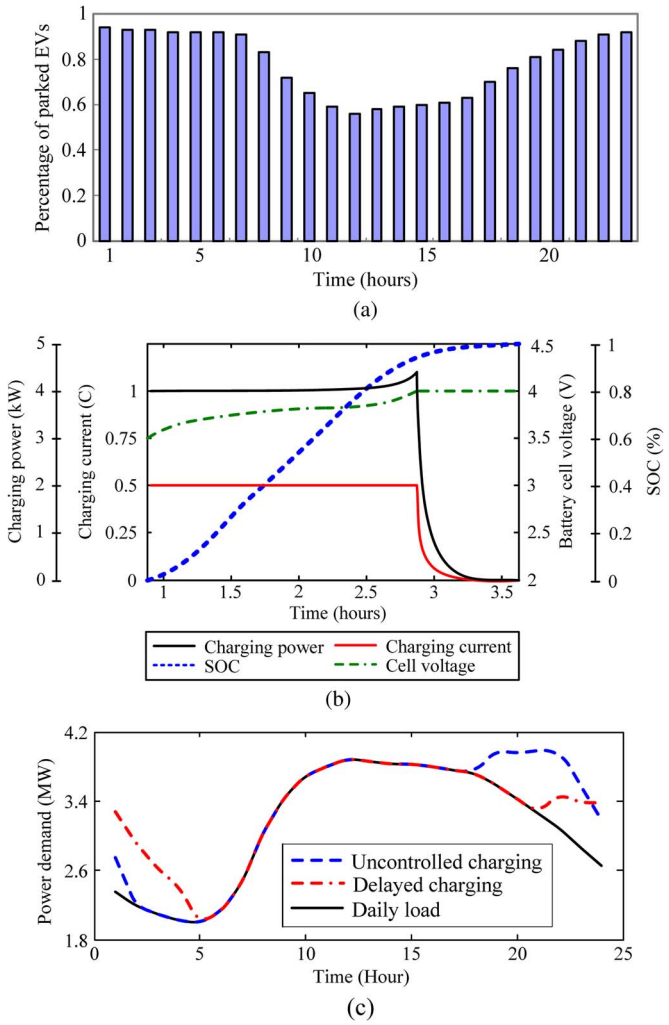

Fig. 2. EV charging period and charging load. (a) Probability of an EV to be parked. (b) EV battery charging profile (Li-ion). (c) Overall EV power consumption under uncontrolled charging and delayed charging scenarios.

that the EVs are connected to the power grid when they return home. The scheduled period is selected as 9 h from 7:00 P.M. to 5:00 A.M. Apart from the estimated charging period, the V2G power is constrained by the power capacity of charging facilities [13]. For home charging, the EVs are connected to the household power outlet and limited by the maximum charging rate.

To formulate the EV charging load, the power and energy required for fully charging the battery are calculated. The EV penetration degree, power level, and the energy storage of the onboard battery pack are listed in Table I. The expected energy consumption of EV charging load is expressed by

$$\varepsilon_T = \sum_{i=1}^{N_{\mathrm{EV}}} \frac{(\mathrm{SOC}_{i,\mathrm{ed}} - \mathrm{SOC}_{i,\mathrm{int}})\mathrm{EC}_i}{\eta} = \frac{\mu(\mathrm{SOC}_{\mathrm{ed}}) - \mu(\mathrm{SOC}_{\mathrm{int}})}{\eta} N_{\mathrm{EV}} \left(\sum_{i=1}^{N_{\mathrm{EC}}} \mathrm{EC}_i \gamma_i \right) \quad (1)$$

where ε_T is the expected energy consumption for charging all EVs, N_{EC} denotes the number of different EV types with EC_i being the power capacity of EV type i, γ_i is the ratio of this EV type, $\mathrm{SOC}_{\mathrm{int}}$ and $\mathrm{SOC}_{\mathrm{ed}}$ represent the initial state of charge (SOC) and the target SOC before departure, η denotes the

TABLE I
SIMULATION PARAMETERS FOR EV FLEETS

Description	Value	Unit
Power level 1– 120V, 15A (Home charging)	1.4	
Power level 2– 240V, 30A	6	kW
(limited by on-board charger)	3.3	
HEV battery capacity	2	kW
PHEV battery capacity	10	kW
EV battery capacity	24	kW
Charging efficiency	0.9	---
Expected number of EVs	1000	Vehicles

power efficiency of the EV charging facility, and N_{EV} denotes the number of EVs that are engaged in the V2G control scheme. It is set to 1000, and the ratios of different EV types are equally shared for the simulation purpose. The required energy roughly equals 10% of the average daily load.

The initial values of SOC at all EV aggregations are considered to follow the same probability density function [13]. A normal distribution $N(\mu, \sigma)$ is used to generate the SOC when an EV starts plugging into the grid, with X being the initial battery SOC, i.e.,

$$X = \mu + \sqrt{2}\sigma \,\mathrm{erf}^{-1}(2p-1), \qquad p \in (0,1) \tag{2}$$

where μ and σ are the mean and variance of the normal distribution, and erf^{-1} is the inverse error function with probability p.

The locations of the EV buses are selected through a random number generator. The six buses between no. 1 and no. 33 are generated as $\{l_1, \ldots, l_6\}$. The ratio of the energy consumption at each bus is produced in a similar way. Namely, $\{r_1, \ldots, r_6\}$ are randomly generated, and the energy consumption of EV aggregation x is calculated by

$$\varepsilon_x = \varepsilon_T \frac{r_x}{\sum_{x=1}^{n_x} r_x}. \tag{3}$$

The constant-current constant-voltage charging method is commonly adopted to prolong the battery lifespan. A typical charging profile for the lithium-ion (Li-ion) battery is shown in Fig. 2(b) [14]. Thus, the EV charging power and energy storage can be estimated using the charging profile during the whole EV parking period. The EV charging load can be shifted to off-peak hours by using the delayed charging strategy, in which the start time for charging for the early arrived EV is postponed for 3 h. The power consumption under the uncontrolled charging and delayed charging are shown in Fig. 2(c). It can be observed that the resulting peak load is increased with uncontrolled EV charging, but a simple delayed charging tactic can curtail the overall peak load.

III. VEHICLE-TO-GRID REGULATION FOR COST MINIMIZATION

A. Formulation of V2G Optimization Problem

A V2G energy scheduling method is proposed to minimize the overall operating cost of the distribution grid where a large portion of electricity is produced by wind power. The total operating cost (TOC) of this power grid can be expressed as

$$\begin{aligned}\mathrm{TOC} = &\sum_{t}^{H}\sum_{g_i}^{N_g} F_i(P_{g_i,t}) + \sum_{t}^{H}\sum_{g_i}^{N_g} F_i(Q_{g_i,t}) \\ &+ \sum_{t}^{H}\sum_{\mathrm{DG}_i}^{N_{\mathrm{DG}}} \left(a_i P_{\mathrm{DG}_i,t}^2 + b P_{\mathrm{DG}_i,t} + c\right) \\ &+ \sum_{\mathrm{EV}_i}^{N_{\mathrm{ev}}}\sum_{t}^{H} r_{\mathrm{EV}_i,t} P_{\mathrm{EV}_i,t} \\ &+ \sum_{\mathrm{EV}_i}^{N_{\mathrm{ev}}} \rho_{\mathrm{EV}_i}\left(\mathrm{EL}_{\mathrm{EV}_i} - \sum_{t}^{H} P_{\mathrm{EV}_i,t}\right) \\ &+ \sum_{t}^{H}\sum_{i}^{N_{\mathrm{ES}}} \rho_{\mathrm{cap}} P_{\mathrm{ES}_i}\end{aligned} \tag{4}$$

where the first component is the cost of electricity purchased from the transmission network with $P_{g_i,t}$ being the power injected to the distribution grid through the substation located at bus i. The injected reactive power at the time index t is denoted $Q_{g_i,t}$, and $F_i(Q_{g_i,t})$ is the price paid for reactive power supply [15]. The third component represents the operating cost of distributed generator i with the supplied power $P_{\mathrm{DG}_i,t}$ at time t. The cost regarding EV charging and V2G services are presented in the fourth and fifth terms, respectively. $r_{\mathrm{EV}_i,t}$ denotes the revenue paid for providing V2G regulation with $P_{\mathrm{EV}_i,t}$ being the power output of the ith EV aggregation when participating in V2G regulation. The penalty for not meeting the battery charging requirement is computed with ρ_{EV_i} being the price for unserved electricity, and $\mathrm{EL}_{\mathrm{EV}_i}$ is the amount of electricity to fully charge EVs by the end of the charging period. The cost for reserve capacity to accommodate the volatile renewable energy generation is represented by the last term of (4), with ρ_{cap} being the price and P_{ES_i} being the regulation power of the ith installed energy storage facility.

Customers are offered multiple electricity tariffs by the utilities to encourage the consumption shift from on-peak to off-peak periods. This paper adopts a double-tariff structure, composed of a high daytime tariff and a low night tariff for different timeslots of a day [2], [16]. In addition to two time-of-use rates on normal days, a critical peak pricing (CPP) is imposed to offset the maximum peaks that only occur on "critical days" in a year [16]. Since the reactive power is not billed in the electricity pricing, the corresponding cost in (4) is set to zero. Thus, the first two components with respect to the cost of purchased energy in (4) can be expressed as

$$\begin{aligned}&\sum_{t}^{H}\sum_{g_i}^{N_g} F_i(P_{g_i,t}) \\ &\quad = \begin{cases} \displaystyle\sum_{t}^{H} \rho_{\mathrm{pk},t} \sum_{g_i}^{N_g} P_{g_i,t} & t \in (8:00, 22:00) \\ \displaystyle\sum_{t}^{H} \rho_{\mathrm{off},t} \sum_{g_i}^{N_g} P_{g_i,t} & \text{other time on normal days} \\ \displaystyle\sum_{t}^{H} \rho_{\mathrm{cpp},t} \sum_{g_i}^{N_g} P_{g_i,t} & \text{critical peak hours} \end{cases}\end{aligned} \tag{5}$$

where $\rho_{\mathrm{pk},t}$ and $\rho_{\mathrm{off},t}$ are the peak tariff and the off-peak tariff of time t, respectively, and $\rho_{\mathrm{cpp},t}$ is the electricity price of critical peak hours.

EVs are preferably charged at night to absorb the excessive wind power, and arranged to feed power back to the grid to level the peak load. By virtue of EV battery storage, those expensive distributed generators such as diesel generators can be excluded from the normal operation; thus, the operating cost of the distributed generators described in (4) can be eliminated if the cost for wind power is assumed zero as the wind power aggravates the variation of the daily load profile so that the peaking generation units and spinning reserves are deployed for regulation up and regulation down services. Thus, a penalty term for overload and oversupply is introduced to reflect the cost induced by the regulation capacity. Since only one price is practically given for positive regulation and negative regulation in many energy markets, one V2G revenue is considered in (4) for V2G energy scheduling, which can be rewritten as

$$\begin{aligned}\mathrm{TOC} = &\sum_{t}^{H}\rho_t\sum_{g_i}^{N_g}P_{g_i,t}+\sum_{t}^{H}\rho_{\mathrm{ol}}(P_{g_i}-P_{\mathrm{up}})\\&+\sum_{t}^{H}\rho_{\mathrm{os}}(P_{\mathrm{lp}}-P_{g_i})+\sum_{\mathrm{EV}_i}^{N_{\mathrm{ev}}}r_{\mathrm{EV}_i}\sum_{t}^{H}P_{\mathrm{EV}_i,t}\\&+\sum_{\mathrm{EV}_i}^{N_{\mathrm{ev}}}\rho_{\mathrm{EV}_i}\left(\mathrm{EL}_{\mathrm{EV}_i}-\sum_{t}^{H}P_{\mathrm{EV}_i,t}\right)\end{aligned}\tag{6}$$

where p_{ol} and p_{os} are the penalty price for overload and oversupply, respectively; and P_{up} and P_{lp} are the upper and lower boundaries of the power demand, respectively.

The objective function $\mathrm{Min}(\mathrm{TOC})$ is subjected to the following constraints. The power balance constraint is expressed as

$$P_{g,t}=\sum_{\mathrm{EV}_i}^{N_{\mathrm{ev}}}P_{\mathrm{EV}_i,t}+\sum_{\mathrm{WG}_i}^{N_{\mathrm{WG}}}P_{\mathrm{WG}_i,t}+\sum_{L_i}^{N_b}P_{L_i,t}+P_{\mathrm{loss},t}\tag{7}$$

where $P_{g,t}$, $P_{Li,t}$, and $P_{\mathrm{loss},t}$ are the generation power, load power, and power losses, respectively; and the power output of EV fleets and wind power generators are denoted $P_{\mathrm{EV}_i,t}$ and $P_{\mathrm{WG}_i,t}$, respectively. Meanwhile, the power output limits for EV power regulation are given by

$$P_{\mathrm{EV},\min}\le p_{\mathrm{EV}_i}(t)\le P_{\mathrm{EV},\max}\tag{8}$$

$$0\le E_{\mathrm{EV}_i,\mathrm{int}}+\int p_{\mathrm{EV}_i}(t)\,dt\le E_{\mathrm{EV}_i,\max}\tag{9}$$

where $p_{\mathrm{EV}_i}(t)$ is the charging or discharging rate of the EV aggregation i; $P_{\mathrm{EV}_i,\max}$ and $P_{\mathrm{EV}_i,\min}$ are the upper and lower boundaries of the EV charging/discharging power, respectively; and $E_{\mathrm{EV}_i,\max}$ and $E_{\mathrm{EV}_i,\mathrm{int}}$ are the maximum and initial energy storage of the EV aggregation i, respectively. The energy stored in the battery should always maintain between zero and the maximum capacity.

The expected value of energy absorbed is the integral of V2G power, which is given by

$$\int p_{\mathrm{EV}_i}(t)\,dt=E_{\mathrm{EV}_i,\max}-E_{\mathrm{EV}_i,\mathrm{int}}\tag{10}$$

TABLE II
SIMULATION PARAMETERS FOR POWER GRID

Grid parameters		System parameters	
$P_{i,\max}$	420 kW	ρ_{EVi}	0.6 \$/kWh
$P_{i,\min}$	60 kW	$\rho_{pk,t}$	0.2 \$/kWh
$Q_{i,\max}$	600 kVar	$\rho_{off,t}$	0.1 \$/kWh
$Q_{i,\min}$	20 kVar	$\rho_{cpp,t}$	0.6 \$/kWh
$R_{l,\max}$	1.068 p.u.	p_{ol}	0.02 \$/kWh
$R_{l,\min}$	0.0575 p.u.	p_{os}	0.02 \$/kWh
$X_{l,\min}$	0.8457 p.u.	P_{up}	(1+10%) P_G
$X_{l,\min}$	0.0393 p.u.	P_{lp}	50% P_G
$P_{EV,\max}$	3 kW	$F_{cpi,\max}$	0.95
$SOC_{\mathrm{int}}^{(mean)}$	20%	$F_{cpi,\min}$	0.65

where $E_{\mathrm{EV}_i,\max}$ and $E_{\mathrm{EV}_i,\mathrm{int}}$ are determined based on the power capacity, the scale of EV aggregation, and the SOC increment. The charging energy limits are governed by

$$\begin{aligned}\mathrm{SOC}_{\min}\le\mathrm{SOC}_{id}(t)\le\mathrm{SOC}_{\max}\\ \mathrm{SOC}_{id}(H)\ge\mathrm{SOC}_{\mathrm{final}}\end{aligned}\tag{11}$$

which indicates that the SOC in each EV should not be lower than $\mathrm{SOC}_{\mathrm{final}}$ at the end of the charging period and varies within the usable range from $\mathrm{SOC}_{\min}$ to $\mathrm{SOC}_{\max}$. In this case, the three SOC values are set to 80%, 0%, and 100%, respectively. The expected increment of energy storage in the aggregation can be calculated by

$$E_{\mathrm{EV}_i}(t)=\sum_{id=1}^{N_{\mathrm{EV}_i}}(\mathrm{SOC}_{id}(t)\mathrm{EC}_{id})\,F_{\mathrm{cp}_i}\tag{12}$$

where SOC_{id} and EC_{id} represent the SOC and the battery capacity of EV id, respectively; N_{EV_i} is the total number of vehicles in the ith EV aggregation; and F_{cp_i} denotes the compensation factor to account for unplanned departures of EVs during the scheduled period.

The optimization problem can be readily solved by using the solvers provided in the MATLAB optimization toolbox. In this case study, the optimal EV power over the charging period is obtained by using the interior point method.

B. Stochastic Optimal Control Algorithm

The parameters adopted for simulation are mainly taken from the previous studies [1], [2], and [5], as listed in Table II. The compensation factors for unplanned departure are uniformly distributed in the interval [0.65, 0.95]. The number of EVs distributed at different buses indicates the size of each EV aggregation. In real situation, the ratio should be measured in accordance with the actual capacity of EV charging infrastructure. In this case, a random number sequence {11 16 14 13 9 6} is used in the simulation. The V2G power capacity exhibits a high degree of diversity in the location, temporal availability,

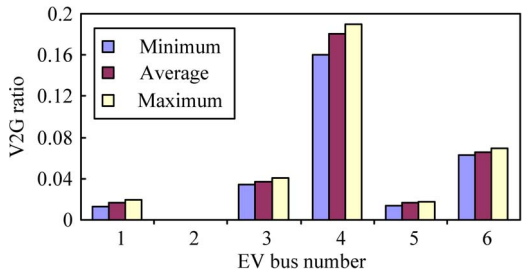

Fig. 3. V2G ratio at different locations.

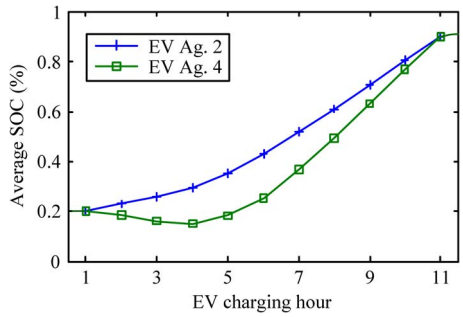

Fig. 4. Average SOC variation at different locations.

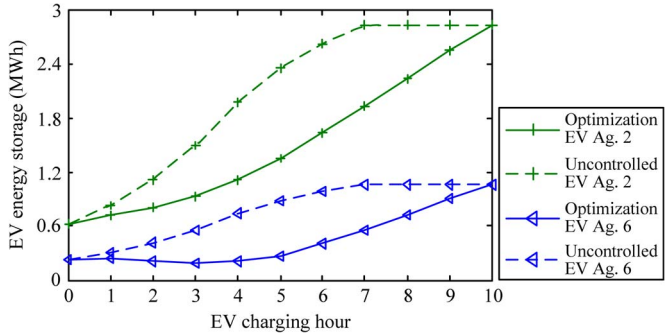

Fig. 5. Energy storage over the charging period for two EV aggregations under uncontrolled scenario and V2G optimization.

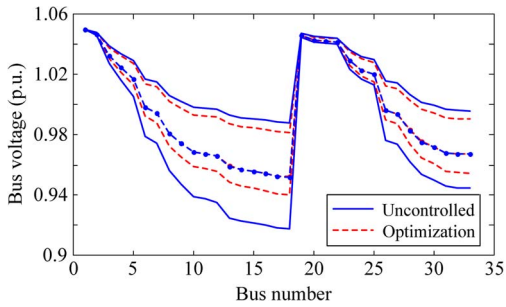

Fig. 6. Maximum, minimum, and average bus voltages during the EV charging period.

and charging demand. Thus, probabilistic analysis is conducted for the proposed optimization problem. The scheduled V2G power at each bus is analyzed by Monte Carlo simulations, where 100 samples of the EV fleet are generated and used. For each simulation, a set of V2G power profile is produced by solving the optimization problem, and the average value is calculated by

$$\overline{P_{\mathrm{EV}_i,t}} = \frac{1}{M}\sum_{j=1}^{M} P_{\mathrm{EV}_i,t}^{(j)} \tag{13}$$

where M is the number of Monte Carlo simulations. An index of the V2G ratio is purposely developed to estimate the power fed back to the grid by discharging EVs at different locations, which is expressed as

$$r_{\mathrm{V2G},i} = \frac{\sum_{d=1}^{D} P_{\mathrm{EV}_i,d}, P_{\mathrm{EV}_i,d} \in \{P_{\mathrm{EV}_i,t} | P_{\mathrm{EV}_i,t} < 0\}}{\sum_{t=1}^{T} P_{\mathrm{EV}_i,t}} \tag{14}$$

where $r_{\mathrm{V2G},i}$ is the V2G ratio of EV aggregation at bus i, and d is the time slot when EVs are scheduled to discharge their batteries. As shown in Fig. 3, the location of EV aggregation in a power network has decisive impact on the V2G ratio, which varies widely depending on the solution of optimal control algorithm. Aggregations 2 and 4 have the biggest disparity and thus are selected to investigate the SOC variation. Fig. 4 shows the average SOC variation of EVs at the two different locations. Although the SOC curves differ due to different charging/discharging processes, the target SOC is achieved by the end of charging period.

C. Analysis of Simulation Results

To evaluate the performance of the optimal control algorithm, the nominal values of variables are taken from Monte Carlo simulations. The operating cost in V2G optimization is \$US 11 940, which is less than the \$US 13 060 in the uncontrolled EV charging scenario. The operating cost is reduced because the demand profile is flattened by V2G energy scheduling, thus avoiding the penalty for overload or oversupply. The electricity cost is also cut down since the peak tariff time is shortened by the peak shaving effect of V2G operation. The EV energy profile over the charging period is shown in Fig. 5. Among EVs aggregated at different distribution feeders, the EV aggregations of largest and smallest sizes are selected to demonstrate the changes in EV energy storage. Both of EV aggregations reach the predefined level of battery energy by the end of the charging period. The bus voltage in the distribution grid is an important factor of power quality, and should be maintained within the standard range [17]. The maximum, minimum, and average values of the bus voltage over the V2G optimization period are plotted in Fig. 6. It can be observed that there is smaller voltage deviation when using V2G optimization.

The participation of EVs in the V2G control scheme in response to different revenues is examined by comparing V2G power output in high and low revenue settings. The changes in the pattern of V2G power regulation for the two selected EV aggregations are plotted in Fig. 7, in which the high revenue is denoted #1 and the low revenue is denoted #2. The EV participation declines as the revenue paid by the distribution system operator (DSO) for V2G control becomes high because the cost associated with V2G power to supply the peak demand

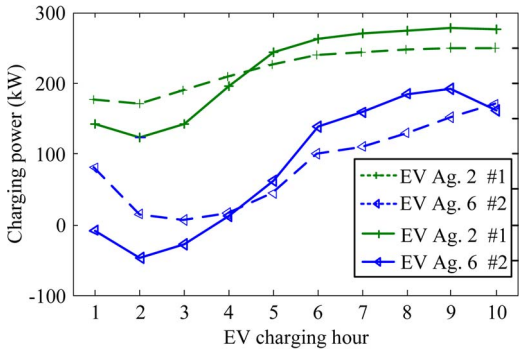

Fig. 7. Comparison of V2G participation with high and low revenues.

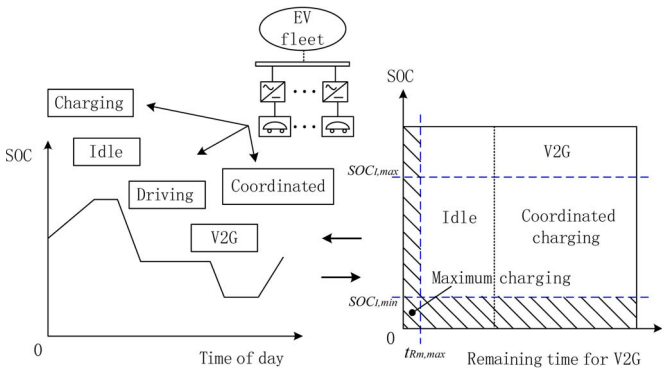

Fig. 8. Power allocation of V2G power aggregation.

is increased. The lower revenue helps bring more EVs into the V2G optimization, but it only offers low incentive to EV owners. Thus, appropriate V2G revenue should be negotiated to ensure the mutual benefits of DSO and EVs contracted to the V2G scheme. The V2G revenue $r_{\mathrm{EV}_i,t}$ must be able to compensate the additional cost on EVs for V2G operation, which is mainly composed of battery degradation and power loss in energy conversion [2], and then should be able to generate additional profit for EV owners. Meanwhile, the DSO can reduce the operating cost by utilizing EV battery energy for load leveling and regulation services.

IV. Vehicle-to-Grid Regulation for Cost Minimization

A. V2G Power Aggregation

EV energy storage can be employed for providing frequency regulation and should get paid in the ancillary service market. The integrated energy management is designed to utilize the EV energy storage to perform V2G cost optimization while effectively stabilizing the frequency. EVs are dispensed into five groups to perform the multifunctional control scheme, and idle EVs are tapped for frequency regulation. As shown in Fig. 8, the group division is mainly determined by the driving pattern, the SOC of onboard battery, and departure time.

- Group I (charging at the maximum rate): The EVs with least remaining time for fully charging a battery before the departure time are dispensed to this group.
- Group II (coordinated charging): EVs with modest energy storage and remaining parking time act as a controllable load to provide the required aggregated V2G power.
- Group III (providing V2G power): V2G operation mode feeds power to the grid; EVs with higher SOC and surplus parking time are eligible for this group.
- Group IV (idle mode): EVs in this group are available for providing ancillary services such as frequency regulation.
- Group V (driving mode): EVs are used for daily commuting and unavailable for any power grid operation.

EVs move between different groups of operation when the parking condition and charging state change. EVs on the top of the list of each operation mode are selected by the aggregator for a specific control scheme. The formulation of each group is expressed as

$$\begin{aligned} g_I = \{&\mathrm{EV}_i | \mathrm{SOC}_{I,\min} \le \mathrm{SOC}_{\mathrm{EV}_i} \le \mathrm{SOC}_{I,\max} \\ &t_{R_m,\min} \le t_{R_m,\mathrm{EV}_i} \le t_{R_m,\max} \text{ and} \\ &r_{F,\mathrm{EV}_i} = 1 \text{ for V2G set}\} \end{aligned} \tag{15}$$

$$\begin{aligned} t_{R_m,\mathrm{EV}_i} = &t_{d,\mathrm{EV}_i} - t \\ &+ \frac{(\mathrm{SOC}_{ed,\mathrm{EV}_i} - \mathrm{SOC}_{\mathrm{EV}_i}(t))\, E_{\mathrm{EV}_i,\max}}{P_{\mathrm{EV}_i,\max}} \end{aligned} \tag{16}$$

where t_{R_m,EV_i} is the remaining time for each parking EV, t_{d,EV_i} is the departure time of the ith EV, $P_{\mathrm{EV}_i,\max}$ is the maximum charging rate, g_I is the ith group of EVs with predefined determinant factors such as the range of SOC and remaining time, and r_{F,EV_i} is the charging facility capable of reversible power transfer.

The workflow of power allocation to each EV is as follows.

1) Formulate Groups I–V according to (15) and (16).
2) Rank the EVs in each group. For Group I, the EVs are ranked according to the remaining time, from the least to the largest. For Group III, the EVs with higher SOC are on the top of the ranking list.
3) Update the group allocation for each time slot, and dispatch EVs from the ranking list. The aggregator serves to match the dispatched V2G power with the hourly optimal solution while fulfilling the target SOC before the departure, i.e.,

$$p_{x_i,k} = p_{x_i,\max}, \text{ if } \mathrm{EV}_i \in \text{Group I} \tag{17}$$

$$\text{if} \quad P_{x,k} > \sum_{i=1}^{i=N_{g_I}} p_{x_i,\max}$$

$$p_{x_i,k} = \frac{P_{x,k} - \sum_{i=1}^{i=N_{g_I}} p_{x_i,\max}}{ng_{II}}, \text{ for } \mathrm{EV}_i \in \text{Group II} \tag{18}$$

$$\text{if} \quad P_{x,k} < \sum_{i=1}^{i=N_{g_I}} p_{x_i,\max}$$

$$p_{x_i,k} = \frac{P_{x,k} - \sum_{i=1}^{i=N_{g_I}} p_{x_i,\max}}{ng_{II}}, \text{ for } \mathrm{EV}_i \in \text{Group III} \tag{19}$$

$$\text{subject to } p_{x_i,\min} < p_{x_i,k} < p_{x_i,\max}, \text{ and}$$

$$p_{x_i,k} = 0, \quad \text{for} \quad t < t_{s,\mathrm{EV}_i} \quad \text{or} \quad t > t_{ed,\mathrm{EV}_i} \tag{20}$$

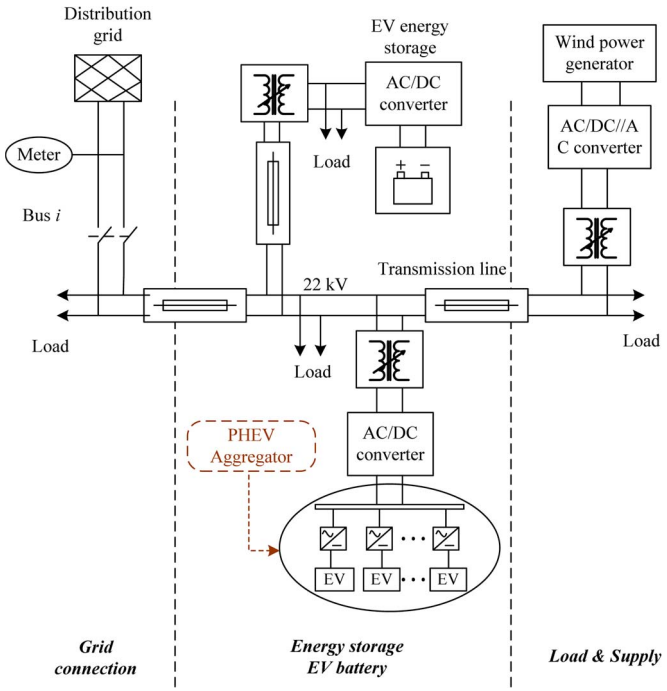

Fig. 9. Schematic diagram of V2G dynamic regulation model with wind power.

where $P_{x,k}$ denotes the scheduled V2G power for EV aggregation x, and $p_{x_i,k}$ denotes the charging/discharging rate for each individual EV.

B. Distributed V2G Power for Frequency Regulation

The EV aggregation close to the terminal of the wind plant can be employed to flatten the generation power, as shown in Fig. 9. The equivalent circuit model is built in simulation to show the current flow of the battery at the connection point [18], [19]. The internal resistance is supposed to be constant during the charge and discharge cycles, in spite of the varying current, and is specified by the battery manufacturer. The battery current, output voltage, and power are calculated as follows:

$$E = E_0 - K\frac{Q}{Q - idt} + A\exp(-Bidt) \tag{21}$$

$$U_{\text{bat}} = E - RI_{\text{bat}} \tag{22}$$

$$P_{\text{bat}} = n_{\text{bp}} U_{\text{bat}} I_{\text{bat}} \tag{23}$$

where E and E_0 represent the battery open-circuit voltage and initial constant voltage, respectively; Q and R denote the battery capacity and internal resistance, respectively; and U_{bat} and I_{bat} are the output voltage and current, respectively. Battery cells are wired in parallel and series so that the battery power is multiplied by n_{bp}.

In the integrated energy management, the solution of V2G optimization P_{EV_i} is used as a parameter of frequency regulation. The total V2G power at each time step should not exceed the capacity of electric equipment such as the rating of transformer tied to the feeder of distribution network, which can be expressed as

$$P_{T_{mi},\min} \le P_{\text{EV}_i}(t) + P_{L_i}(t) + p_f(t) \le P_{T_{mi},\max} \tag{24}$$

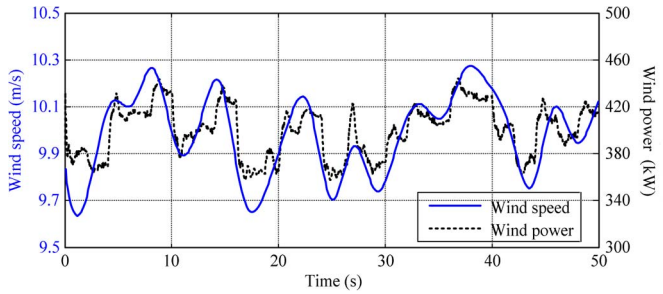

Fig. 10. Wind speed fluctuation and wind power variation.

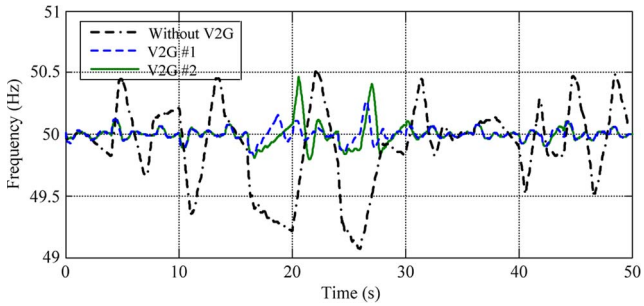

Fig. 11. Frequency deviation with and without V2G dynamic power regulation.

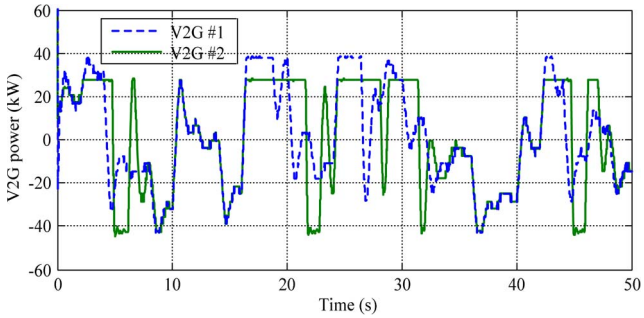

Fig. 12. Power output in V2G frequency regulation.

where $P_{T_{mi},\min}$ and $P_{T_{mi},\max}$ are the upper and lower loading limits of the primary transformer, and $p_f(t)$ is the regulatory power for frequency stabilization.

The continuous variation of wind speed and the corresponding wind power fluctuation are shown in Fig. 10. V2G power capacity is limited in the range of $+/-40$ kW. In the first case, the full V2G capacity is employed. In the second case, the maximum power that EVs can supply to the grid is reduced by 25%, considering the time-varying nature of EV energy storage. The simulation result in the first case is depicted in dotted blue line, whereas the solid green line represents the second case. As shown in Fig. 11, the frequency can be successfully stabilized. The power regulation of EV aggregation in the same timeframe is plotted in Fig. 12. Owing to the alternating EV charging and discharging control in response to frequency swell and sag, the net energy required is almost zero. Thus, the EV energy storage is not affected, and there is no additional battery degradation cost.

C. Implementation of Control Scheme

As shown in Fig. 9, the wind power generator, EVs, and other loads are clustered at a certain bus in the test distribution grid.

TABLE III
CLUSTERED COMPONENTS IN EXPERIMENTAL SETUP

Cluster	Load	Resource	Storage
Apparatus	Electronic load	Controllable power supply	Battery (smart charging&V2G)
Voltage range of DC/DC converter	Max. 350V	Max. 120V	Max. 60V
Voltage rating of component	100V	30V	2*12V
Variable	Current i_{el}	Current i_s	Charger voltage and current
Scheduled range of variation	3-10A	1-5A	10-15V; 0-5A

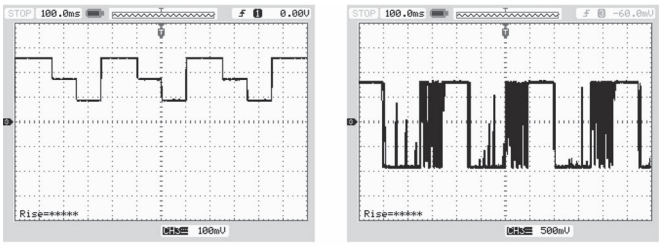

(a) (b)

Fig. 13. Measured instantaneous response of battery pack to sudden change on power output of other components. (a) Output current of electronic load (3.5 A/div, 100 ms/div). (b) Charging current of battery pack (2.5 A/div, 100 ms/div).

As EVs are employed to locally compensate for the power fluctuation caused by neighboring renewable resources, the overall power flow of the cluster can be smoothed, thus eliminating the negative effect on the power quality of the external grid. The experimental setup utilizes the control signal produced by simulation software where the load profile, wind power fluctuation, and corresponding instructions for V2G power are calculated.

A downscaled experimental setup is built to implement the simulation algorithm. Three types of components are electrically connected in the network: the load, the resource, and the battery energy storage. In this case, the electronic load and regulated power supply are used to emulate the load and the varying wind power generation. The experimental condition is listed in Table III. These components are tied to an internal 380-V dc link and connected to the external ac grid through a dc/ac converter. The converter controller is designed to maintain the dc link voltage and regulate the output voltage for each component. Fig. 13 shows the dynamic power regulation of the battery storage in response to the varying load and supply. The instantaneous changes of power supply are measured in Fig. 13(a), and the battery charging/discharging current is presented in Fig. 13(b). The battery is charged to absorb the excessive power supply and is discharged when the demand becomes larger. The power response of the EV battery is captured to demonstrate its capability of reacting appropriately to the wind power fluctuation in real time. The unbalanced power of the network ultimately conveys to the external grid. The power flow at the connecting point during the transition period is presented in Fig. 14. It can be observed that the ac injected into the 220-V electrical power network is distorted

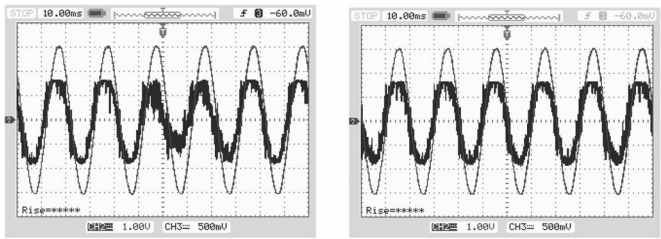

(a) (b)

Fig. 14. Measured voltage and current waveforms at the connecting point of ac power grid (100 V/div, 2.5 V/div, 10 ms/div). (a) Without EV battery compensation. (b) With EV battery compensation.

in Fig. 14(a) due to the abrupt changes of the wind power generation. In contrast, the available EV battery is activated to compensate the same changes in the power network. As shown in Fig. 14(b), the ac power flow can be stabilized when the battery storage is deployed for dynamic power compensation.

V. CONCLUSION

In this paper, the wind power generators and EVs with the capability of V2G operation are integrated in the distribution grid. A mathematical model of V2G power control is formulated, which incorporates EV models into power grid optimization. The V2G optimization method is proposed to schedule the EV charging and discharging energy to minimize the operating cost while satisfying the mobility needs and power system limitations. In addition to V2G optimal energy scheduling, EVs are also deployed for dynamic power regulation, which requires fast response to the instantaneous imbalance between the power supply and demand. V2G power is controlled to mitigate the power fluctuation and, thus, stabilize the system frequency and voltage. The simulation results verify effective utilization of V2G power for multiple purposes. Finally, the hardware-in-the-loop system is developed to implement software simulation by regulating power converters, and the measured results validate the simulation model.

REFERENCES

[1] C. Liu, K. T. Chau, D. Wu, and S. Gao, "Opportunities and challenges of vehicle-to-home, vehicle-to-vehicle and vehicle-to-grid technologies," *Proc. IEEE*, vol. 101, no. 11, pp. 2409–2427, Nov. 2013.
[2] W. Kempton and J. Tomic, "Vehicle-to-grid power fundamentals: Calculating capacity and net revenue," *J. Power Sources*, vol. 144, no. 1, pp. 268–279, Jun. 2005.
[3] A. Y. Saber and G. K. Venayagamoorthy, "Plug-in vehicles and renewable energy sources for cost and emission reductions," *IEEE Trans. Ind. Electron.*, vol. 58, no. 4, pp. 1229–1238, Apr. 2011.
[4] S. Han, S. Han, and K. Sezaki, "Estimation of achievable power capacity from plug-in electric vehicles for V2G frequency regulation: Case studies for market participation," *IEEE Trans. Smart Grid*, vol. 2, no. 4, pp. 632–641, Dec. 2011.
[5] S. Han, S. Han, and K. Sezaki, "Development of an optimal vehicle-to-grid aggregator for frequency regulation," *IEEE Trans. Smart Grid*, vol. 1, no. 1, pp. 65–72, Feb. 2010.
[6] C. C. Chan and K. T. Chau, *Modern Electric Vehicle Technology*. London, U.K.: Oxford Univ. Press, Nov. 2001.
[7] J. J. Escudero-Garzas, A. Garcia-Armada, and G. Seco-Granados, "Fair design of plug-in electric vehicles aggregator for V2G regulation," *IEEE Trans. Veh. Technol.*, vol. 61, no. 8, pp. 3406–3419, Oct. 2012.
[8] N. Rotering and M. Ilic, "Optimal charge control of plug-in hybrid electric vehicles in deregulated electricity markets," *IEEE Trans. Power Syst.*, vol. 26, no. 3, pp. 1021–1029, Aug. 2011.

[9] F. Guo, E. Inoa, W. Choi, and J. Wang, "Study on global optimization and control strategy development for a PHEV charging facility," *IEEE Trans. Veh. Technol.*, vol. 61, no. 6, pp. 2431–2441, Jul. 2012.
[10] V. V. Viswanathan and M. Kintner-Meyer, "Second use of transportation batteries: Maximizing the value of batteries for transportation and grid services," *IEEE Trans. Veh. Technol.*, vol. 60, no. 7, pp. 2963–2970, Sep. 2011.
[11] M. Hosseini, H. A. Shayanfar, and M. F. Firuzabad, "Reliability improvement of distribution system using SSVR," *ISA Trans.*, vol. 48, no. 1, pp. 98–106, Jan. 2009.
[12] U.S. Dept. Transp., Fed. Hwy. Admin., National Household Travel Survey (NHTS). [Online]. Available: http://nhts.ornl.gov/download.shtml
[13] D. Wu, D. C. Aliprantis, and K. Gkritza, "Electric energy and power consumption by light-duty plug-in electric vehicles," *IEEE Trans. Power Syst.*, vol. 26, no. 2, pp. 738–746, May 2011.
[14] *LFP Battery User Manual*, Thunder Sky, Cincinnati, OH, USA, 2010.
[15] W. El-Khattam, Y. G. Hegazy, and M. M. A. Salama, "An integrated distributed generation optimization model for distribution system planning," *IEEE Trans. Power Syst.*, vol. 20, no. 2, pp. 1158–1165, May 2005.
[16] K. Herter, P. McAuliffe, and A. Rosenfeld, "An exploratory analysis of California residential customer response to critical peak pricing of electricity," *Energy*, vol. 32, no. 1, pp. 25–34, Jan. 2007.
[17] *Voltage Characteristics of Electricity Supplied by Public Distribution Systems*, Std. EN50160, 1994, CENELEC Eur. Comm. Electro-technical Stand.
[18] Z. Amjadi and S. S. Williamson, "Prototype design and controller implementation for a battery-ultracapacitor hybrid electric vehicle energy storage system," *IEEE Trans. Smart Grid*, vol. 3, no. 1, pp. 332–340, Mar. 2012.
[19] C. Pang, P. Dutta, and M. Kezunovic, "BEVs/PHEVs as dispersed energy storage for V2B uses in the smart grid," *IEEE Trans. Smart Grid*, vol. 3, no. 1, pp. 473–482, Mar. 2012.

Shuang Gao (S'09) received the B.Eng. and M.Eng. degrees in electrical engineering from Tianjin University, China, in 2007 and 2009, respectively. She is currently working toward the Ph.D. degree in electrical and electronic engineering with The Department of Electrical and Electronic Engineering, University of Hong Kong, Hong Kong.

She currently focuses on the power quality analysis for electric vehicle integration, optimization of vehicle-to-grid systems, and battery energy management. Her research interests include electric vehicle technology, integration of electric vehicles and renewable energy, and energy conversion.

K. T. Chau (M'89–SM'04–F'13) received the B.Sc.(Eng.), M.Phil., and Ph.D. degrees in electrical and electronic engineering from The University of Hong Kong, Hong Kong, in 1988, 1991, and 1993, respectively.

Since 1995, he has been with The University of Hong Kong, where he is currently a Professor with the Department of Electrical and Electronic Engineering and the Director of the International Research Center for Electric Vehicles. He is the author of four books and over 400 refereed technical papers. His research interests include electric and hybrid vehicles.

Dr. Chau is a Fellow of the Institution of Engineering and Technology and of the Hong Kong Institution of Engineers. He currently serves as a Coeditor of the *Journal of Asian Electric Vehicles*. He is a Chartered Engineer. He received the Changjiang Chair Professorship from the Ministry of Education, China, and the Environmental Excellence in Transportation Award for Education, Training, and Public Awareness from the Society for Automotive Engineer International.

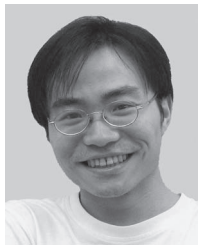

Chunhua Liu (S'05-M'10-SM'14) received the B.Eng. and M.Eng. degrees from Beijing Institute of Technology, Beijing, China, in 2002 and 2005, respectively, and the Ph.D. degree in electrical engineering from The University of Hong Kong, Hong Kong, in 2009.

He is currently serving as an Assistant Professor with the Department of Electrical and Electronic Engineering, The University of Hong Kong. His research interests include energy conversion, integration, and distribution, particularly of electric machines and drives, electric vehicles, renewable energy, wireless power transfer, vehicle-to-grid systems, microgrids, and smart grids.

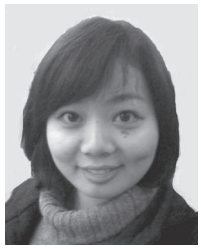

Diyun Wu (S'09) received the B.Eng and M.Eng. degrees in electrical engineering from Tianjin University, China, in 2007 and 2009, respectively. She is currently working toward the Ph.D. degree in electrical and electronic engineering with The University of Hong Kong, Hong Kong.

She is currently focusing on the design of the framework of smart grid with vehicle-to-grid operation, as well as vehicle-to-grid for smart energy delivery. Her research interests include electric vehicles, vehicle-to-grid systems, and power electronics.

C. C. Chan (M'77–SM'77–F'92) received the B. Sc. degree from China University of Mining and Technology, Beijing, China, in 1957; the M.Sc. degree from Tsinghua University, Beijing, in 1959; and the Ph.D. degree from The University of Hong Kong, Hong Kong, in 1982, all in electrical engineering.

He is currently an Honorary Professor with the Department of Electrical and Electronic Engineering, University of Hong Kong.

Dr. Chan is a Fellow of the Royal Academy of Engineering U.K., the first Academician of the Chinese Academy of Engineering in Hong Kong, and a Fellow of the Hong Kong Academy of Engineering Sciences.